Key Engineering Materials
ISSN: 1662-9795, Vol. 926, pp 34-45
doi:10.4028/p-b22a9a

Submitted: 2021-11-30
Accepted: 2022-02-18
Online: 2022-07-22

From Theory to Practice: Development and Calibration of Micro Pellet Extruder for Additive Manufacturing

Albert Curmi[a] and Arif Rochman[b]

University of Malta, Malta

[a]albert.curmi@um.edu.mt; [b]arif.rochman@um.edu.mt

Keywords: Pellet, extrusion, ABS, 3D printing, additive manufacturing, single screw extruder

Abstract. Pellet additive manufacturing (PAM) is in terms of printing process very similar to the widely used fused deposition modelling (FDM) systems. The main difference is the use of pellets instead of filament. In this study, a pellet, single screw extruder is developed. A screw design with variable pitch and depth is modelled analytically to predict the melting behavior of acrylonitrile butadiene styrene (ABS) during steady state extrusion. The extruder screw was designed unconventionally short with a length of 85 mm and a diameter of 20 mm, giving an L:D ratio of 4.25:1. The model predicted the melting profile for ABS being extruder at 235°C at 10 RPM, the result of which was confirmed to a degree by experimentation. The extrusion rate of the screw extruder was measured at barrel temperatures of 225°C to 245°C with 5°C increments and at 5 RPM and 10 RPM. The extrusion was found to increase non-linearly with barrel temperature and screw speeds. The extruder printed adequately on an FDM style motion system with minor upgrades.

Introduction

Fabricating a product can be challenging especially if it is a bespoke item of limited to no previous production. This barrier limited the ingenuity of designers for millennia and has led to great efforts to attenuate were possible the challenges therein. Additive manufacturing is the latest and arguably the most accessible technology to ease the constraints set when fabricating an item.

Additive manufacturing incorporates any manufacturing method which joins materials, layer by layer, in a controlled fashion to fabricate a desired product. Material extrusion is one of the most popular additive manufacturing techniques in use [1], having become common place in most engineering spaces, especially for prototyping. One such example is a Fused Deposition Modelling (FDM) 3D printer, which is relatively cheap, the lower end models going at $300 or even less. This has made FDM machines widely available and accessible to a wide audience. An FDM 3D printer works by melting thermoplastic in filament form and then extruding and depositing it layer by layer to produce the desired part. FDM is not only cheap and cost-effective but it is also simple to operate, reliable and easily customizable [2]. Nonetheless, it is not a perfect system the main issues being lack of material variety, low production speeds, low accuracy and quality, relatively high material costs and limited acceptability in highly regulated fields such as fabrication of biomedical devices [1].

Pellet based additive manufacturing (PAM) provides a solution to some of the aforementioned issues. PAM employs pellets instead of filament as the material source in use whilst fabricating the desired geometry. Using pellets inherently leads to a much wider material library which may be applied to the same equipment with minimal changes necessary. Pellets are also cheaper, coming at least 2.5 times cheaper than their filament counterpart [3]. If a screw is employed as the main plasticizing element of the extruder, additives may be incorporated in the feedstock to alter the material properties as desired. Furthermore, screw extruders are capable of large material throughput which may result in faster printing speeds, given a correct setup.

Small format pellet 3D printers present a difficult challenge to design due to the inherent weight and size of a conventional pellet extruder. The size of the raw material to be extruded controls the size and weight of the extruder. The smaller the raw material, the smaller the extruder can be but also the more difficult it is to obtain the materials and often these come at a higher cost compared to the common industrial pellets. The smallest extruders developed to the knowledge of the author use either

powders [4], [5], shredded polymer flakes or thinly chopper filament [3]. In some cases, raw polymer pellets may be produced by the manufacturer in a relatively small format, such as the polycaprolactone (PCL) pellets used by Liu et al. which allowed the researchers to use a small 14 mm diameter screw [6]. The smaller the screw diameter, the shorter the screw needs to be and therefore the smaller the overall extruder.

When using pellets as the raw material source it is difficult to downscale an extruder to a format similar in size to that of a filament 3D printer. Studies carried out by Reddy et al., Tseng et al. and Zhou et al. each developed pellet 3D printing systems which were relatively bulky compared to a conventional filament driven extruder [7]–[9]. Each research group has used different screw diameters, Tseng et al. employed a 14 mm diameter and 280 mm long screw whereas Zhou et al. used a 12 mm diameter and 206.4 mm long screw. The screw to diameter ratio is of 20 and 17.2 respectively [7], [9]. These long screws ensure that the pellets are well molten and plasticized in the extruder whilst providing enough pressure to push material out of the nozzle. The main challenge is that these extruders are relatively bulky, which means that they may not be applied to use on a common place FDM desktop motion system, thus limiting their use.

The aim of this work is to propose a small format, short, pellet, screw extruder which can work with relatively large pellets and has a small size and weight. The main objectives are to: (1) design a screw and predict its melting rate using an analytical model; (2) develop the remaining components to suit the screw; (3) manufacture the parts required and test the screw extruder; (4) compare the observed melting rate with the predicted one; (5) use the system developed for actual 3D printing on a conventional FDM motion system.

Theory

A conventional thermoplastic single extrusion screw is composed of three definite sections as shown in Figure 1, namely: feeding, compression, and metering sections. The first research published which studied the melting behavior in a screw extruder can be attributed to Maddock [10]. His work involved performing screw-freezing experiments where a screw was pulled-out when operating steadily to measure the actual melting behavior of the thermoplastic therein. From his observations, Maddock noted that the polymer first melts as a thin film at the interface between the solid pellets (solid bed) in the screw channel and the heated barrel. This thin film is actively dragged by the rotating screw and pushed downwards towards the leading flight of the screw, as shown in Figure 2. A melt pool is formed in this region which builds up pressure and in turn compresses the solid bed, thus actively decreasing its width. The height of the solid bed remains relatively constant throughout the whole process.

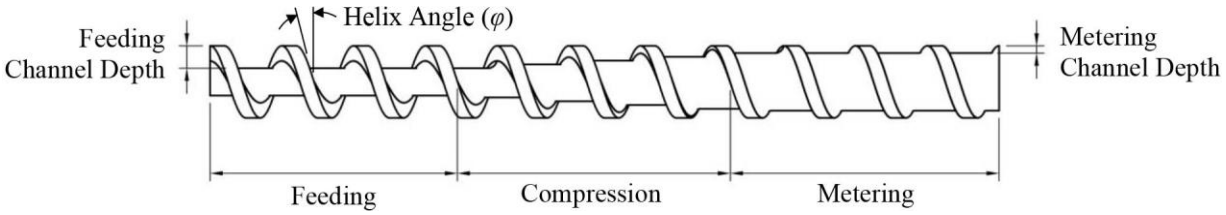

Figure 1 – Square pitch extrusion screw diagram showing channel depth and helix angle with screw section.

Years later, Tadmor developed his first analytical model of melting behavior using the data presented by Maddock [11]. This model describes the melting process shown in Figure 2, where W is the width of the screw channel, X is the solid bed width, H is depth of the channel and δ is the melt film thickness. It should be noted that not all polymers observe this melting process with notable exceptions such as Polyvinylchloride (PVC), Polypropylene (PP) and Low-density polyethylene (LDPE) [12].

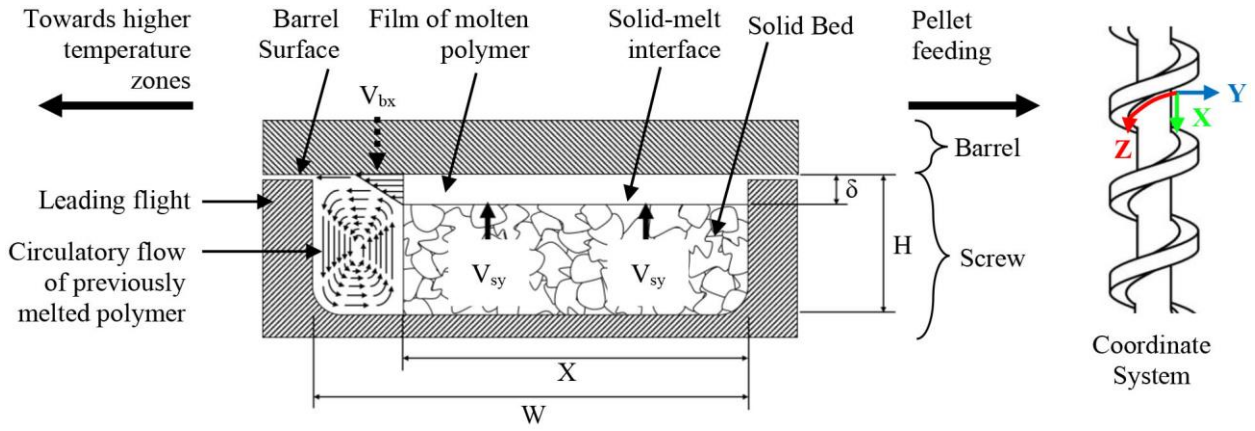

Figure 2 - Model diagram of the drag induced melting mechanism in screw channel cross-section with coordinate system.

Tadmor further refined and validated his work with multiple successive publications [13]–[15]. Subsequent researchers that continued to develop the original model aimed to decrease its main simplifying assumptions. These works along with the group's own studies led Mount et al. to argue that the Tadmor model erroneously predicted the melting rate and only by coincidence could it predict the solid-bed profile [16]. The profile prediction is significantly related to the calculation used to determine the solid bed velocity [17]. The crux of the problem was that the Tadmor model assumes a constant solid-bed velocity along the length of the screw which is known to be incorrect. In practice, the velocity will change due to tapering screw sections, changes in barrel temperature, and the decreasing depth of the screw channel towards the metering section.

This work will nonetheless apply the non-isothermal drag flow of a power law fluid model described by Tadmor and Gogos in their latest known publication which dealt with the most poignant issues of the original model [12]. Better predictions may be obtained when applying a finite element simulation to specific regions of the extrusion process [17]. This would involve simulating the solid conveying region in the feeding section, and the melting process that occurs thereafter. The latter generally requires a separate model for the feeding, compression, and metering sections respectively. The usefulness of the Tadmor model lies within its approachability and that is the main reason this work will evaluate its predictions when applied to a short extrusion screw meant for additive manufacturing.

The equations listed from Eq. (1) to Eq. (17) describe the Tadmor analytical model for the melting rate and solid bed profile in a single screw extruder [12]. This model assumes that there exists a steady state in which the velocity and temperature of the thermoplastic at any given cross-section of the extruder screw are constant with time. The solid bed is assumed to be homogenous and continuous. The cross-section of the screw channel is assumed to be a rectangle, i.e. the channel is not filleted and has sharp corners. Melting is assumed to take place solely at the surface in contact with the barrel which is taking part in a drag-induced melt removal mechanism. This model does not take note of the non-linear temperature profile in the melt film nor the effect of flight clearance between the screw and barrel. The latter assumption is generally the most significant [12], i.e. the wider the gap, the greater the amount of melt that will flow through that gap, also known as leakage flow. The leakage flow in a conventional single screw extruder is often deleterious as the material is not efficiently pumped out of the screw. Furthermore, the material has relatively large shear rate given the small gap leading to localized high temperatures and possible material degradation. On the other hand, leakage provides a degree of mixing, albeit small [18].

The rate of melting is defined by Eq. (1) where V_b is the barrel speed (m/s), ρ_m is the melt density (kg/m^3), k_m is the thermal conductivity of the polymer (W/m°C), T_b is the barrel temperature, T_m is the melting temperature of the polymer, X is the solid bed width, λ is heat of fusion (J/kg), C_s and C_m are the polymer's heat capacity in solid and molten form respectively (J/kg°C). By removing the root of the solid bed width ($\sqrt{X}$) from Eq (1), the term Φ can be defined by Eq. (2) which is a useful simplification for later calculations.

$$w_L(x) = \sqrt{\frac{V_{bx}\rho_m U_2\left[k_m(T_b-T_m)+\frac{U_1}{2}\right]X}{2[\lambda+C_s(T_m-T_{s0})+C_m\bar{\Theta}(T_b-T_m)]}} = \Phi\sqrt{X}. \quad (1)$$

$$\Phi = \sqrt{\frac{V_{bx}\rho_m U_2\left[k_m(T_b-T_m)+\frac{U_1}{2}\right]}{2[\lambda+C_s(T_m-T_{s0})+C_m\bar{\Theta}(T_b-T_m)]}}. \quad (2)$$

The melt film thickness δ (mm) is found using Eq. (3). The terms U_1 (N/s) and U_2 are defined in Eq. (4) and (5) respectively. U_2 represents the reduction of the rate of melt removal by drag flow. This may be caused by the change in viscosity brought about by a change in temperature along with the shear thinning behavior of a given material. $U_1/2$ represents the rate of viscous dissipation per unit width in the melt film. The $k_m(T_b - T_m)$ term in Eq. (2) represents the heating by conduction in the material. Therefore, by comparing the former and latter terms just described, one would compare the viscous dissipation and heat conduction also known as the Brickman Number (Br) as shown in Eq. (6).

$$\delta = \sqrt{\frac{[2k_m(T_b-T_m)+U_1]X}{\rho_m V_{bx} U_2[\lambda+C_s(T_m-T_{s0})+\lambda+C_m\bar{\Theta}(T_b-T_m)]}}. \quad (3)$$

$$U_1 = 2m_0 V_j^{n+1}\bar{\delta}^{1-n}\left(\frac{e^{-b\prime}+b\prime-1}{(b\prime)^2}\right)\left(\frac{b\prime}{1-e^{-b\prime}}\right)^{n+1}. \quad (4)$$

$$U_2 = \frac{2(1-b'-e^{-b\prime})}{b\prime(e^{-b\prime}-1)}. \quad (5)$$

$$Br = \frac{U_1}{2k_m(T_b-T_m)}. \quad (6)$$

The term b' may be found using Eq. (7) where a and n are terms which make part of the viscosity for a power-law fluid model as shown in Eq. (8), where T (K) is the temperature of the material, $\dot{\gamma}$ is the shear rate (1/s), n is the power law index and a and m_0 are both co-efficient of viscosity. The b' term is also required to calculate the mean temperature $\bar{\Theta}$ of the melt film as shown in Eq. (9).

$$b' = \frac{-a(T_b-T_m)}{n}. \quad (7)$$

$$\eta = m_0 e^{-a(T-T_m)}\dot{\gamma}^{n-1}. \quad (8)$$

$$\bar{\Theta} = \frac{\frac{b\prime}{2}+e^{-b\prime}\left(1+\frac{1}{b\prime}\right)-\frac{1}{b\prime}}{e^{-b\prime}+b'-1}. \quad (9)$$

The down channel velocity V_{sz} (m/s) of the solid bed may be found with Eq. (10), where G is the solid mass flow rate (kg/s) and ρ_s is the material solid density (kg/m^3). This is the weakest aspect of the Tadmor model as discussed previously. The barrel velocity V_b (m/s) is found using Eq. (11), where N is the rotational speed of the screw (RPM) and D_b is the barrel diameter (mm). The more useful cross-channel barrel velocity V_{bx} (m/s) is found using Eq. (12) where φ is the helix angle of the screw. The absolute difference between the barrel velocity and the velocity of the solid bed is V_j and is found using Eq. (13).

$$V_{sz} = \frac{G}{\rho_S HW}. \quad (10)$$

$$V_b = \pi N D_b. \quad (11)$$

$$V_{bx} = V_b \sin\varphi = \pi N D_b \sin\varphi. \quad (12)$$

$$V_j = \overrightarrow{V_b} - \overrightarrow{V_{sz}} = \sqrt{{V_b}^2 + {V_{sz}}^2 - 2V_b V_{sz}\cos\varphi}. \quad (13)$$

For the feeding and metering sections, both of which have a constant depth, Eq. (14) may be used to calculate the solid bed profile (X/W), where X_1 (mm) is the previous solid bed width at Z_1 (mm), z

(mm) is the current coordinate and ψ is a dimensionless number calculated using Eq. (16). Similarly, the solid bed profile (*X/W)* of the compression section may be found using Eq. (15), where *A* is the taper co-efficient calculated using Eq. (17) and H_1 is the previous channel depth.

$$\frac{X}{W} = \frac{X_1}{W}\left[1 - \frac{\psi(z - Z_1)}{2H}\right]^2. \tag{14}$$

$$\frac{X}{W} = \frac{X_1}{W}\left\{\frac{\psi}{A} - \left[\left(\frac{\psi}{A} - 1\right)\sqrt{\frac{H_1}{H}}\right]\right\}^2. \tag{15}$$

$$\psi = \frac{\Phi}{V_{sz}\rho_s\sqrt{X_1}}. \tag{16}$$

$$A = \frac{dH}{dZ} = \frac{H_1 - H_2}{N_{turns}\left(\frac{D_b}{\sin\varphi}\right)}. \tag{17}$$

The derivation of Eq. (1) to (17) may be found throughout the works published by Tadmor [12]–[15].

The model was coded using Python 3 programming language with Jupyter Lab and Jupyter Notebook programming environments. The Tadmor model was calculated using the order shown in Figure 3, which follows the general indications set by Tadmor with the exception that the helix angle φ may be altered along the length of the screw. A change in φ leads to a change in velocity of both the barrel and the solid bed and therefore these parameters have to be recalculated every iteration down the length of the screw along with the usual parameters (U_1, Φ, ψ, δ, *X/W*).

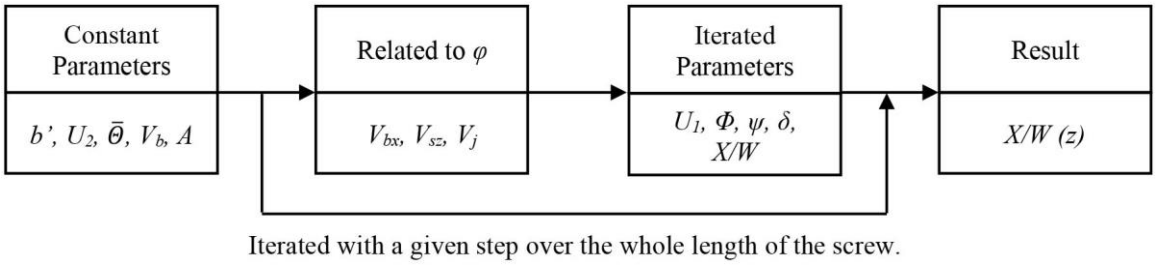

Figure 3 - Calculation flow of Tadmor model with consideration for varibale helix angle.

Materials and Method

Materials. The extruder was tested using acrylonitrile butadiene styrene (ABS) pellets (P2H-AT) from ELIX POLYMERS, La Canonja, Spain, which is an easy flowing, high gloss, and injection molding grade ABS. It is marketed to have a standard impact toughness and includes antistatic additives. The ABS did not have any added colorants and had a natural ivory color.

Analytical Modelling. The screw was modelled using the modified Tadmor model implemented in Python, which allows for a variable helix angle. The main parameters of the extrusion screw are shown in Table 1, and all lengths provided are axial and not helical. For each parameter, the compression section provides a linear transition from feeding to metering parameters. Since the helix angle is not constant, the compression ratio was calculated by comparing the helical cross-sectional area of the feeding and compression section, resulting in a ratio of 1.4:1. The flight thickness was set to 1.5 mm and is measured helically and not parrel to the axis of the extrusion screw.

The length of the screw was kept as small as possible, at 85 mm, so that the extruder would have a similar size to an FDM extruder. The diameter of the screw was set to 20 mm to allow for a deep feeding section capable of taking most pellet size, even those at the larger end of the spectrum. The screw was designed with a small starting helix angle of 13° at the feeding section which then transitions to 17° at the metering section. For comparison, a conventional square pitch screw extruder would have a helix angle of about 17.657° which is equivalent to a pitch equal to the diameter of the screw.

Table 1 – Geometric specifications of extrusion screw

	Length [mm]	Turns	Helix Angle [°]	Depth [mm]
Feeding Section	21.25	1.46	13	6.0
Compression Section	42.50	2.54	-	-
Metering Section	21.25	1.11	17	3.3

The ABS for extrusion was modelled according to the power law model presented in Eq. (8). The power law index n, melting temperature T_m and the co-efficient m_0 and a were found by fitting the power-law model to viscosity-shear rate graphs provided by the manufacturer.

All of the process parameters are listed in Table 2. The screw speed N and mass flow rate G were determined by experimentation on the working extruder. The material feeding temperature T_{s0} was set at a common room temperature value of 25°C. The thermal conductivity k_m, solid heat capacity C_s and molten heat capacity C_m were found from literature, given that the supplier did not provide this information. The melt density ρ_m was assumed to be 1170 kg/m^3 at any point in the process. The value is ballpark figure taken from literature [12]. The heat of fusion was set to 0 given that ABS is amorphous and therefore does not have a clear solidification phase change therefore this value does not apply. The melting process was assumed to start 1 turn down the extrusion screw. The model was increment with a step of 0.1 turns.

In one modelling session, the barrel temperature was varied in between 225°C and 245°C with 5°C steps. In another study, the barrel temperature was kept constant, but the screw speed was decreased to 5 RPM and the solid mass flow rate G was decreased to 0.164 kg/s to reflect the change in speed.

Table 2 - Processing parameters for modelling

Symbol	Unit	Value	Symbol	Unit	Value
T_b	°C	235	k_m	W/m.°C	0.205
N	RPM	10	C_s	kJ/kg°C	1.189
G	kg/hr	0.28	C_m	kJ/kg°C	1.863
T_{s0}	°C	25	ρ_m	kg/m3	1170

Screw Warm-Push Test. The screw described in the previous section was manufactured and assembled into an extruder. The barrel of the screw was heated using a spring, resistance heater and the temperature was measure at the nozzle using a PT100 temperature sensor supplied by E3D (England). The screw was driven by a geared 30:1 NEMA 17 stepper motor 17HS15-1684S-HG30 from Stepper Online (Jiangning Nanjing, China). The motor was mounted inline with extruder, but it may also be mounted on the side to decrease the aspect ratio of the extruder. The feeding end of the screw was kept cool throughout the whole process.

Given the geometry of the extruder, the screw has to be pushed out of the barrel for disassembly. The system was let to extrude until the material output, if any, was continuous. This was considered as the extruder reaching its steady state and then it was let to cool to room temperature. Next the barrel was heated slowly whilst periodically trying to push the screw out. Eventually the screw was dislodged and pulled out gently. The temperature was set lower than the usual processing temperature. Using this technique decreases the smearing of molten material from the metering and compression section onto the feeding section. Doing so would decrease the usefulness of the result as the start of melting would be less clear.

The ABS was dislodged and removed from the extrusion screw. The pellets and initial solidified material in the feeding section and start of compression section were difficult to preserve and study given that they were very fragile. These were disregarded in the present study. The remaining material was split in 5 cross sections per turn. Each cross section was sliced using a Diamond WireTec DWS175 (Germany) Diamond Wire Saw and the sections were viewed using a Remet Nikon SMZ-2T Stereomicroscope (Japan) with a Leica DFC295 (Germany) digital color camera.

Extrusion Rate at Different Temperatures. The extruder was set at the desired temperature and left to stabilize. Next, two extrusion regimes were carried out with three repeats, first at 5 RPM for 5 screw turns and then at 10 RPM for 10 screw turns. This test was done using temperatures between 225°C and 245°C with 5°C increments. For each repeat, the extruded material was weighted on a PS 1000.3Y, Radwag (Poland) precision balance.

Assembly of Extruder on 3D Printer and Tuning. The extruder was mounted on a conventional CR-10s by Creality (China) which had upgraded Z axis motors to take the extra weight. The Z stepper motors were changed from two BJ45D14-26V02 with a rated torque of 0.4 Nm each to two 17HS19-2004S1 stepper motors from Stepper Online (Jiangning Nanjing, China) with a rated torque of 0.59 Nm each. Furthermore, in the new set-up, the Z-steppers each had an independent stepper driver, unlike in the original set-up which used one stepper driver connected in parallel, to provide the required current.

The GCODE for the 3D printer controller was made using PrusaSlicer by Prusa Research (Prague, Czech Republic). To the author's knowledge all of the opensource programs available are meant for filament 3D printers and do not have a specific version for pellet extruders. The main parameter of note to bridge the gap, is the extrusion multiplier which is used to control how much material is extruded for a given movement. The extrusion multiplier may be set to an equivalent value so that a certain material flow rate is obtained for a given rotation of the screw extruder.

To determine the correct extrusion multiplier, PrusaSlicer was used to generate a simple GCODE which printed a single outer wall perimeter of a 30 mm square, 3 layers high. The first layer is squashed to improve bed adhesion and therefore is not a good indicator to correct the extrusion rate, whereas the third layer should be relatively plane and is better suited for the task. The width of the third track was measure using Remet Nikon SMZ-2T Stereomicroscope (Japan) with a Leica DFC295 (Germany) digital color camera, on each side and the average was taken as the track width w_0. This value was then compared to the target width w_t and the original extrusion multiplier Em_0 using Eq. (18) to obtain a better extrusion multiplier Em_1. The process may have to be repeated if the original extrusion multiplier was significantly off or the extrusion process was not stable enough. Test was carried using a 1 mm nozzle, with 80 mm/s printing speed and at a barrel temperature of 235°C.

$$Em_1 = Em_0 \times \frac{w_T}{w_0}. \tag{18}$$

3D Printing Complex Models. The Benchy [19] was 3D printed to verify the capabilities of the extruder but also as a reference for further tuning. It was sliced as shown in Figure 7 (a) and (b). This model is popular within the 3D printing community and therefore it is simple to compare and troubleshoot. The model was sliced in PrusaSlicer to generate the GCODE for the 3D printer movements. The slicing parameters were left similar to those set on a Creality CR-10 3D printer, except for the extrusion multiplier as discussed previously. The speeds were also increased to 80 mm/s for perimeters and infill whereas for external perimeters and top solid infill, it was set to 40 mm/s. The layer cooling was set to maximum and a 1 mm nozzle was used for 3D printing.

Results

Analytical Modelling and Screw Warm-Push. The material model for ABS is shown in Figure 4 which presents the data provided by the supplier compared with the power law model. The power law fitting shown in Figure 4 was made using points in the shear rate region generally employed in an extrusion process, i.e. from 100 to 1000 (1/s). The power law model should be applied to the injection molding shear rate range, i.e. from 1000 to 10000 (1/s) where the exponential decrease in viscosity is correctly modelled using power law. This approach would be incorrect as it would make the model overestimate the actual viscosity present in the process.

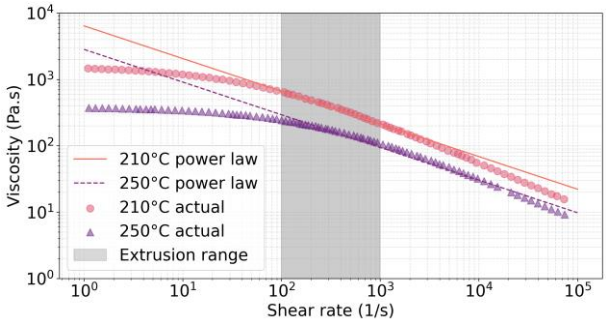

Parameter	Value*
m_0	6417
n	0.51
a	0.0204
T_m	210°C

(*) for a shear rate range of conventional extrusion between 100 s^{-1} and 1000 s^{-1}

Figure 4 - Viscosity vs Shear rate graph of ABS P2H-AT with manufacturer data and power law model along with the numerical value of the power law model parameters.

The most relevant results of the analytical model are shown in Figure 5. The solid lines in both Figure 5 (a) and (b), shows the same result given that it follows the parameters listed in Table 2 and may be considered as the reference. The vertical lines labelled as *section change* mark the transition points from feeding to compression section and from compression to metering section. An X/W value of 0 would signify that the pellets have completely melted at that point. The shear rate increases at the metering section because theoretically the melt film thickness decreases significantly. In practice, at that point the screw section would be mostly melted and therefore the shear rate value presented in inconsequential. The Br number is relatively constant and set at a low value, throughout the whole extrusion process.

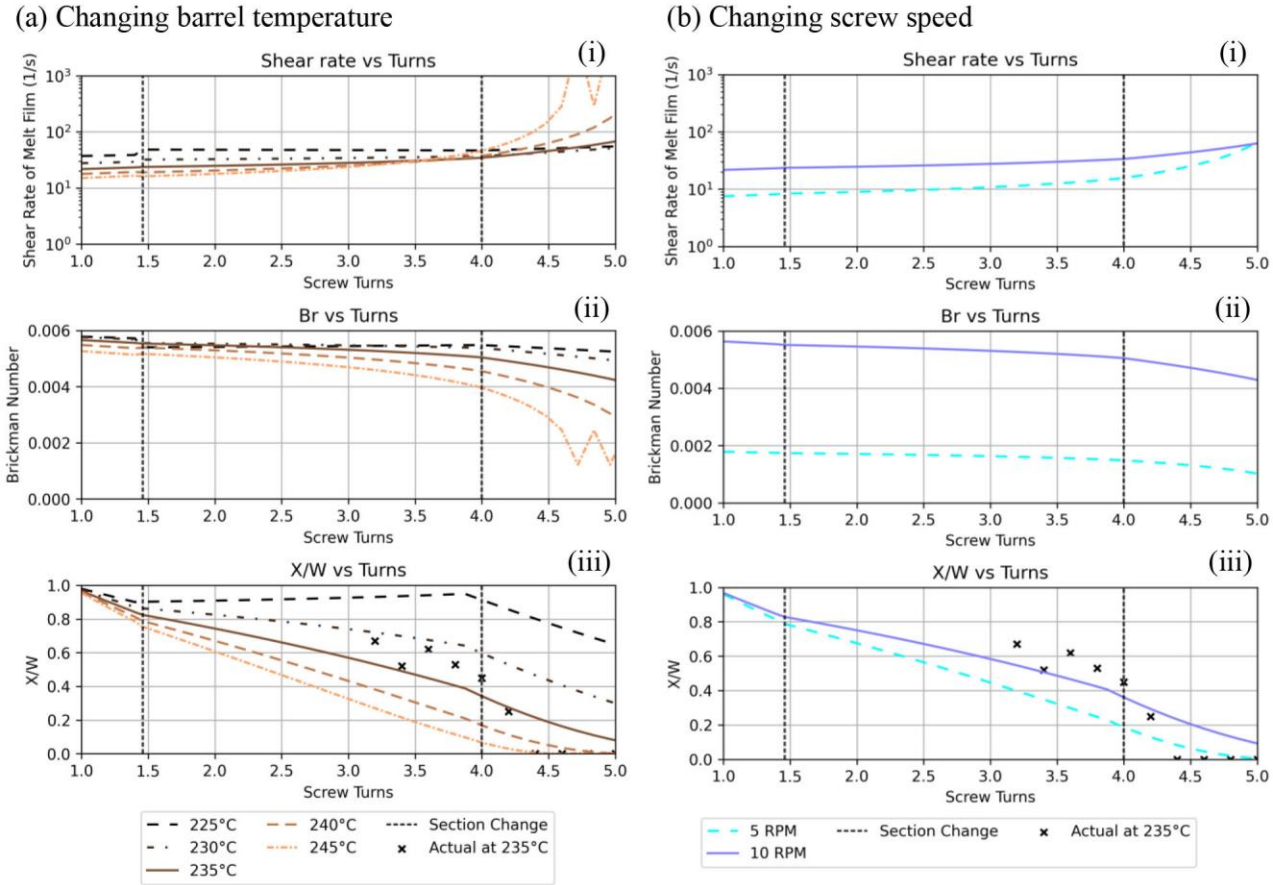

Figure 5 - Plots of shear rate of melt film (i), Brickman number (ii) and solid bed profile (X/W) (iii) vs the screw turns from feeding section to metering section, with: (a) varying barrel temperature and (b) varying screw rotational speed, using 100 to 1000 s^{-1} shear rate power law model.

The actual melting profile (*X/W*), measured at 235°C, 10 RPM is superimposed on the analytical predictions of Figure 5 (iii), and shows a moderate agreement in the compression section. The solidified polymer cross-sections are shown in Figure 6. The sections between turns 4.4 to 5 are not

shown as they would show a fully molten polymer just like turns 4.4 and 5. The whitening, outlined with a dashed line, predominantly visible in the cross-section of turn 4.4 and to a lesser extent in cross-sections of turns 3.6 and 5 are due to bending of the ABS caused during removal from screw and cutting, which elongates it and causes the marks. Incompletely molten material is ivory-white in color and does not show as parallel lines, whereas molted material is a dark ivory color.

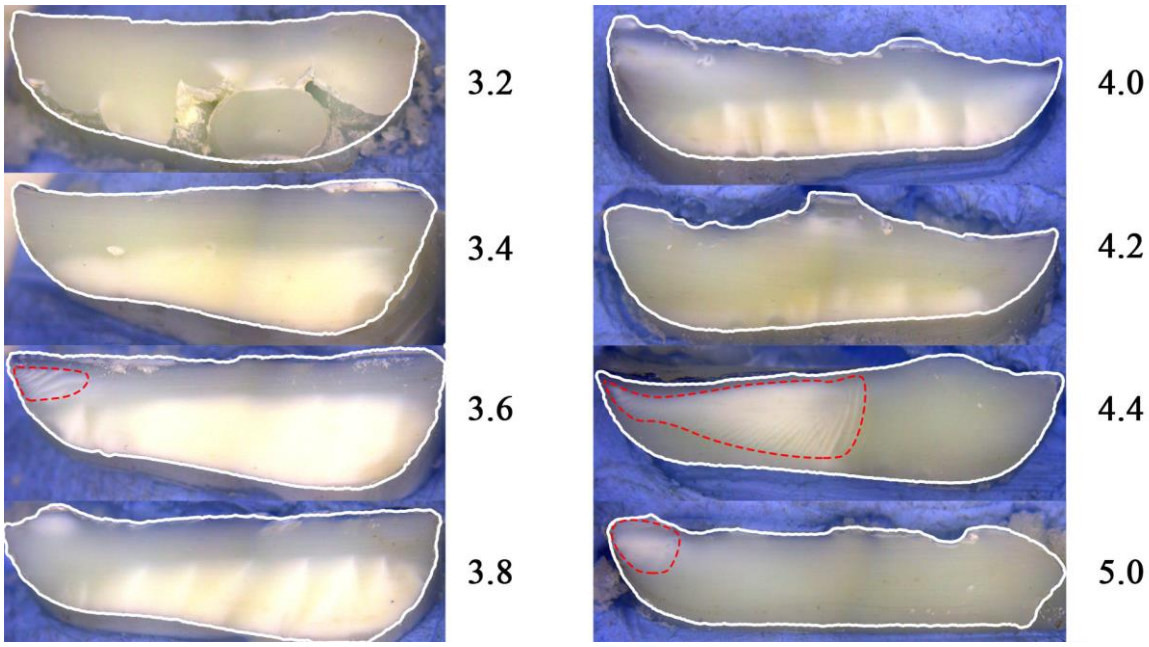

Figure 6 - Cross-section of solidified ABS derived from screw warm push-out test, sliced face outlined in white and each is annoted with screw turn position.

Extrusion Rate and Multiplier. The extruder was capable of extruding continuously at temperatures above 235°C. Temperatures below this value led to two forms of failure, either by excessive polymer viscosity which would lead to insufficient stepper motor power to drive the screw or else plugging of the polymer in the screw, making the extruder rotate without extrusion. Going sufficiently beyond 245°C increase the propensity for polymer degradation.

The best operating temperature was found to be 235°C, given that Pit is the lowest temperature which does not have any issues associated with excessive viscosity, nor is there any visible burning or degradation in some form of the ABS. As shown in Table 3, increasing the temperature and the rotational speed of the screw leads to an increase in extrusion rate. In both cases, the increase is not linear, which is expected given that the change in viscosity is not linear and this in turn has a controlling effect on the extrusion process. The multiplier value refers to the result obtained when dividing the extrusion rate at 10 RPM with that at 5 RPM. In a linear relationship, the value would be expected to be 2 or thereabout.

The extrusion multiplier was found to be 0.37, with the slicer set for a filament of 1.75 mm. Using this value, the parts produced were found to be dimensionally correct. The calibration test had to be carried out three times to get a correct result.

Table 3 - Extrusion rate results for different temperatures and screw speeds.

Temperature [°C]	Extrudate [g]						Extrusion Rate [g/s]		Multiplier
	5 RPM for 5 turns			10 RPM for 10 turns			5 RPM	10 RPM	
	1	2	3	1	2	3			
235	2.489	2.716	2.737	4.736	4.548	4.428	0.0441	0.0762	1.73
240	2.564	2.763	2.861	4.550	4.391	5.018	0.0455	0.0776	1.70
245	2.763	2.918	2.911	4.857	5.313	5.062	0.0477	0.0846	1.77

3D Printing. The extruder performed adequately whilst 3D printing and produced a Benchy of relatively good quality considering that a 1 mm nozzle was used. The simulated, model along with some close-up photos of the 3D printed part are shown in Figure 7 (a) and (b).

One of the most prominent issues noted is insufficient shape retention of the deposited layers caused by delayed solidification. This issue led to a rough surface finish, most visible on the hull of the boat. Another symptom of this problem are the imperfect overhangs created, such as the top of windows and doors of the Benchy, best shown in Figure 7 (e) and (f). The issue is somewhat exacerbated by the thick 0.5 mm layer height, usually making the model more prone to such defects. The chimney at the top end of the Benchy, shown in Figure 7 (c) and (d) was mostly a failure, which is reasonable given that this region is the most sensitive to insufficient shape retention.

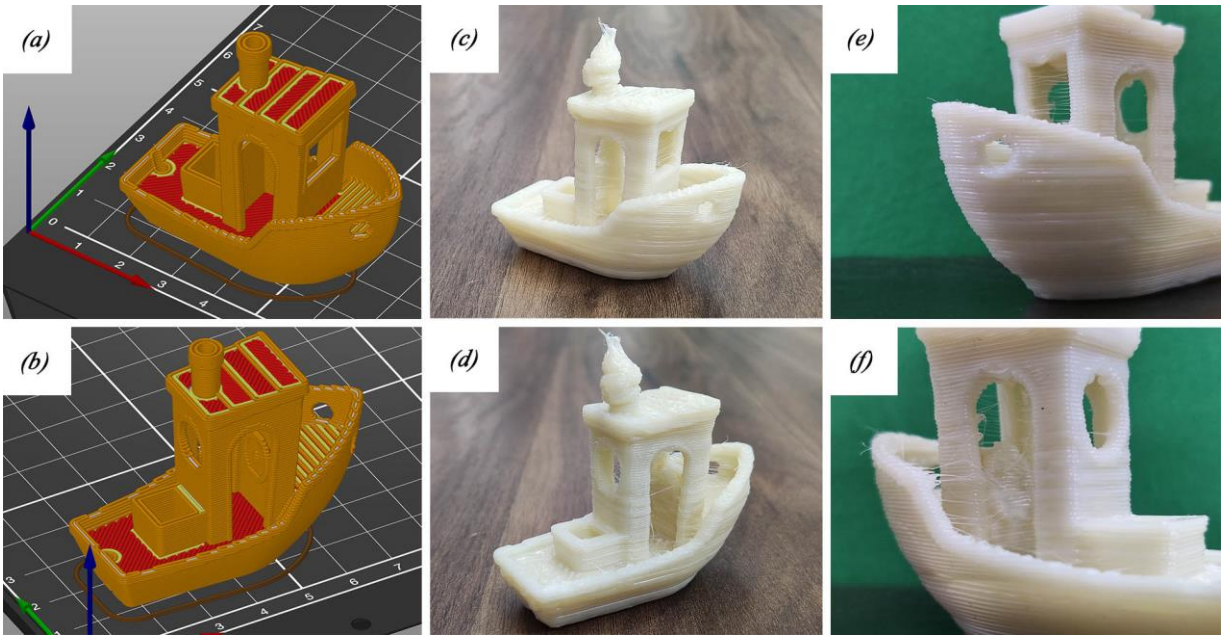

Figure 7 - (a) and (b) Simulation of 3D printed Benchy from two different angles. One base square is equal to 1 cm. (c) to (f) 3D printed Benchy using injection molding grade ABS

Discussion

Relevance of the Modified Tadmor Model. The results shown in Figure 5 are useful in a number of ways. At a preface value, these results provide an indication of the sensitivity of the extrusion process to changes in temperature and screw rotational speed. On the other hand, the result was not completely representative of what was actually observed in practice. The model failed to predict the early complete melting observed in the metering zone but the melting rate of the compression section was very similar to the experimental result. This problem agrees to some degree with the observations of Mount et al. stated earlier, in the sense that the Tadmor model is not best suited to accurately predict the solid bed-profile [16].

Nonetheless, the value of the model, especially when applied to unusually low L:D ratio screws for additive manufacturing, lies in its ability to preemptively showcase possible issues with a given design. For example, for the given screw geometry, the model predicted that operating at 225°C and 230°C would likely mean that the extruder would not sufficiently melt the ABS, as shown in Figure 5 (a)(iii) and therefore extrusion would fail. The extrusion study confirmed this prediction as it showed that extrusion was not possible at that temperature as the stepper motor could not turn the screw continuously due to the excessive resistance caused by the high melt viscosity.

The experimental results provided have an inherent error. The early melting observed in the metering section may have been caused by the method used to extract the screw from the barrel. Given that the barrel had to be heated slightly to pull out the screw so as not to damage the equipment, it is expected that the material may have melted some more, even beyond the outer shell of the screw and thus distorted the results. This effect would be more prevalent in the metering section as it is

usually the most heated as the cooling applied to feeding end creates a thermal gradient to the metering end. Nonetheless, it is the author's opinion, that this effect is improbable given that the barrel temperature was kept at about 140°C and for a very short period of time.

The model also gave an indication of the effect of decreasing screw speed, predicting a higher melting rate. In most conventional extruders, increasing speed would increase melting rate due to greater shearing. In this case, it is expected that due to the higher residency time of the thermoplastic in the extruder, the material would be more molten.

The result of the model also indicates that the Br number is low, close to 0, as shown in Figure 5 (a)(ii) and (b)(ii). A low Br number indicates that heating is mostly done conductively by the resistance heaters rather than by shearing. This is as expected given that the rotational speed is very low and therefore shearing is limited. The shear rate is set within the 1 s^{-1} to 100 s^{-1} range which is well below the conventional extrusion range. Nonetheless, it is not unusual as most extrusion processes operate at much larger throughputs and speeds than those applied in this process.

The solid bed profile observed in practice was not the same as that observed by Maddock, upon which the whole model is built. The cross-sections shown in Figure 6 do not have a clear melt pool as observed by Maddock on his significantly larger screw extruders. The solid bed profile is apparently compressed by an ever-thickening top layer of molten material. The heat transferred from the barrel, melts the solid bed from the top and then the heat keeps travelling down towards the root of the channel until it melts all of the material therein. To confirm or refute this description, the screw push-out test would have to be repeated but this time using dyed pellets so that any mixing that may be occurring would be better visualized. A similar strategy was used by Maddock in the original screw pull tests he pioneered [10].

Extrusion Consistency and 3D Printing. A consistent and predictable extrusion rate is necessary for good quality 3D printing. The predictions of the Tadmor model shown in Figure 5 and the extrusion test results shown in Table 3 tell of a relatively consistent extrusion but which changes non-linearly with temperature and screw rotational speed.

During normal 3D printing, the temperature is kept relatively constant, with maximum possible fluctuations of about 1°C ever so often. Shifting the temperature by 5°C did show a change in extrusion rate, but even at 5°C the change was not that significant therefore it is expected that a 1°C change would only show as a minor imperfection in the surface quality of most 3D prints. More importantly, the presence of this effect indicates that any tuning done to determine the extrusion multiplier should be carried out at the desired printing temperature.

The issue becomes more relevant when dealing with screw speed whilst extruding and 3D printing. Usually, the slicer is set to print outer layers slowly, for better positional accuracy, whereas the internal structures would be printed faster to reduce the overall production time. In such a scenario the internal structure would invariably be over extruded relative to the external structure. Oftentimes this issue is not significant as the material being deposited has ample empty space where it can be shifted to. Therefore, extrusion multiplier tuning should be carried out using outer perimeters rather than any internal features, as done in this study, if dimensional accuracy and aesthetics are valued.

The PAM 3D printed Benchy shown in Figure 7 (c) to (f) shows a rather consistent extrusion profile. The insufficient shape retention makes it difficult to clearly determine whether any particular defect is down to inconsistent extrusion or otherwise. More cooling is required for shape retention.

Conclusion

The Tadmor analytical model for single screw extruders is applicable to small L:D ratio extrusion screws intended for additive manufacturing. The predictions achieved by the model are not exact and may need a correction due to the low level of shearing during additive manufacturing, which inherently makes the process heavily dependent on heat conducted from the heating barrel. A variable depth and pitch extrusion screw with a L:D ratio of 4.25:1 is applicable to be used in an extruder for PAM. The extrusion rate increases in a non-linear fashion if the temperature of the barrel or rotational speed of the screw is increased. PAM extruders may be miniaturized to a format similar in size to FDM.

Acknowledgement and Funding

The authors thank all partners involved in the MALTI3D project for their continuous support. The MALTI3D research project was funded by the Malta Council for Science and Technology through the FUSION: R&I Technology Development Programme (R&I-2018-009T)

References

[1] C. F. Durach, S. Kurpjuweit, and S. M. Wagner, "The impact of additive manufacturing on supply chains," International Journal of Physical Distribution and Logistics Management, vol. 47, no. 10, pp. 954–971, 2017, doi: 10.1108/IJPDLM-11-2016-0332.

[2] Z. Jiang, B. Diggle, M. L. Tan, J. Viktorova, C. W. Bennett, and L. A. Connal, "Extrusion 3D Printing of Polymeric Materials with Advanced Properties," Advanced Science, vol. 7, no. 17. John Wiley and Sons Inc., Sep. 01, 2020. doi: 10.1002/advs.202001379.

[3] A. Alexandre, F. A. Cruz Sanchez, H. Boudaoud, M. Camargo, and J. M. Pearce, "Mechanical Properties of Direct Waste Printing of Polylactic Acid with Universal Pellets Extruder: Comparison to Fused Filament Fabrication on Open-Source Desktop Three-Dimensional Printers," 3D Printing and Additive Manufacturing, vol. 7, no. 5, pp. 237–247, Oct. 2020, doi: 10.1089/3dp.2019.0195.

[4] B. M. Boyle, P. T. Xiong, T. E. Mensch, T. J. Werder, and G. M. Miyake, "3D printing using powder melt extrusion," Additive Manufacturing, vol. 29, Oct. 2019, doi: 10.1016/j.addma.2019.100811.

[5] J. L. Dávila, M. S. Freitas, P. Inforçatti Neto, Z. C. Silveira, J. V. L. Silva, and M. A. D'Ávila, "Fabrication of PCL/β-TCP scaffolds by 3D mini-screw extrusion printing," Journal of Applied Polymer Science, vol. 133, no. 15, Apr. 2016, doi: 10.1002/app.43031.

[6] S. Liu, P. Zhao, S. Wu, C. Zhang, J. Fu, and Z. Chen, "A Pellet 3D Printer: Device Design and Process Parameters Optimization," Advances in Polymer Technology, vol. 2019, pp. 1–8, Nov. 2019, doi: 10.1155/2019/5075327.

[7] J. W. Tseng et al., "Screw extrusion-based additive manufacturing of PEEK," Materials and Design, vol. 140, pp. 209–221, Feb. 2018, doi: 10.1016/j.matdes.2017.11.032.

[8] B. v. Reddy, N. v. Reddy, and A. Ghosh, "Fused deposition modelling using direct extrusion," Virtual and Physical Prototyping, vol. 2, no. 1, pp. 51–60, Mar. 2007, doi: 10.1080/ 17452750701336486.

[9] Z. Zhou, I. Salaoru, P. Morris, and G. J. Gibbons, "Additive manufacturing of heat-sensitive polymer melt using a pellet-fed material extrusion," Additive Manufacturing, vol. 24, pp. 552–559, Dec. 2018, doi: 10.1016/j.addma.2018.10.040.

[10] B. Maddock, "A visual analysis of flow and mixing in extruder screws," SPE ANTEC Tech. Papers, vol. 15, pp. 383–389, 1959.

[11] Z. Tadmor, "Fundamentals of Plasticating Extrusion," Polymer Engineering and Science, pp. 185–190, 1966.

[12] Z. Tadmor and C. G. Gogos, Principles of Polymer Processing, 2nd ed. Hoboken, New Jersey: John Wiley & Sons, Inc., Publication, 2006.

[13] E. Broyer and Z. Tadmor, "Solids Conveying in Screw Extruders Part I: A Modified Isothermal Model," Polymer Engineering and Science, vol. 12, no. 1, pp. 12–24, 1972.

[14] Z. Tadmor and E. Broyer, "Solids Conveying in Screw Extruders Part II: Non Isothermal Model"," Polymer Engineering and Science, vol. 12, no. 5, pp. 378–386, 1972.

[15] Z. Tadmor, I. Duvdevani, and I. Klein, "Melting in Plasticating Extruders Theory and Experiments," Polymer Engineering and Science, pp. 198–217, 1967.

[16] E. M. Mount and C. 1 Chung, "Melting Behavior of Solid Polymers on a Metal Surface at Processing Conditions," Polymer Engineering Science, vol. 22, pp. 729–737, 1978.

[17] A. Altinkaynak, M. Gupta, M. A. Spalding, and S. L. Crabtree, "Melting in a single screw extruder: Experiments and 3D finite element simulations," International Polymer Processing, vol. 26, no. 2, pp. 182–196, 2011, doi: 10.3139/217.2419.

[18] C. Rauwendaal, Polymer extrusion: Fifth edition. 2014. doi: 10.3139/9781569905395.

[19] Creative Tools, "3DBenchy - The jolly 3D printing torture-test." https://www.3dbenchy.com/ (accessed Nov. 24, 2021).